ACS OMEGA

Open Access

http://pubs.acs.org/journal/acsodf

Article

Loss of Volatile Metabolites during Concentration of Metabolomic Extracts

Nataliya A. Osik, Nikita N. Lukzen, Vadim V. Yanshole, and Yuri P. Tsentalovich*

Cite This: *ACS Omega* 2024, 9, 24015−24024

Read Online

ACCESS | Metrics & More | Article Recommendations | Supporting Information

ABSTRACT: Volatile metabolites can be lost during the preanalytical stage of metabolomic analysis. This work is aimed at the experimental and theoretical study of mechanisms of volatile substance evaporation and retention in the residues during the drying of extract solutions. We demonstrate that solvent evaporation leads to the unavoidable loss of nondissociating volatile metabolites with low boiling points and high vapor pressures (such as acetone and ethanol). The retention of dissociating volatile compounds (primarily organic acids RH) during the evaporation depends on the presence of buffer salts in solution, which are responsible for maintaining the neutral pH. An acid remains in the solution as long as it is present predominantly in the dissociated R^- state. At the very last stage of solvent evaporation, buffer salts precipitate, forming a solid matrix for metabolite trapping in the residue. At the same time, buffer precipitation leads to a decrease of the solution pH, increase of the portion of RH in associated state, and acceleration of RH volatilization. The RH recovery is thus determined by the competition between the solute volatilization in the associated RH form and metabolite trapping in the solid matrix. The retention of volatile acids in the residue after extract drying can be improved either by adding buffer salts to maintain high pH or by incomplete sample drying.

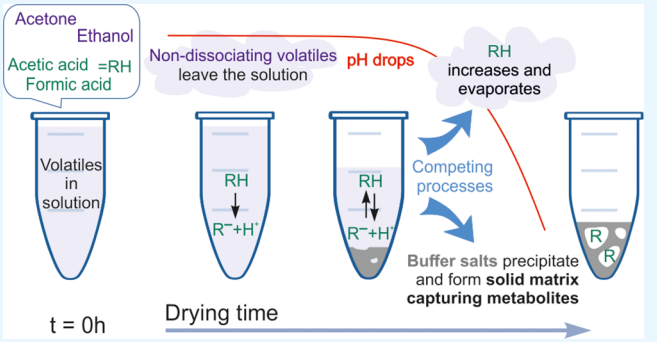

INTRODUCTION

Metabolomics is a relatively young science that is still developing. Its fundamental objectives include the identification, quantification, and characterization of metabolites present in a tissue, organ, or whole body; determining the role of these compounds in a complex biochemical network; and the evaluation of metabolomic changes induced by intrinsic (such as diseases and genetic modifications) or extrinsic (such as environmental variations, diet, and medications) factors. All experiments start with the selection of biological samples, cells, biofluids, or tissues followed by the preanalytical stage. The latter includes sample collection, homogenization, quenching metabolic activity, protein precipitation, and extraction of low-molecular-weight compounds as a separate fraction.[1−4] The analytical step consists of the metabolite detection and quantification, and it is usually performed with the use of such analytical platforms as nuclear magnetic resonance (NMR) spectroscopy, gas or liquid chromatography, and capillary electrophoresis with mass spectrometric detection (GC−MS, LC−MS, or CE−MS).[5−10]

Very often, metabolomic extracts need to be concentrated before analysis. This is primarily required to increase the detection sensitivity as well as to replace the solvent with a more suitable one for the analysis. Drying under nitrogen flow, rotary vacuum evaporation, and freeze-drying (lyophilization) are the most common laboratory techniques for evaporating solvents.[11−13] All drying methods are based on the properties of solvents, which have a high vapor pressure, low boiling point, and high evaporation rate and therefore are volatile, easily volatilized from a liquid or frozen extract. However, extract drying also causes an inevitable loss of volatile biological substances, which also leave the solution during the concentration process.[14−16] This is especially valid for compounds with low boiling points and high vapor pressures (such as acetone, ethanol, acetic, and formic acids). The metabolomic analysis of biological samples often includes these compounds in published data sets.[17−22] Although the effect of metabolite loss under vacuum drying is quite expected, scientists do not always pay much attention to changes in the content of volatiles during the preanalytical step of sample preparation.

Poor recovery of volatiles in the remaining extract may affect the metabolomic profiling of a tissue and lead to incorrect data interpretation. The errors caused by the loss of volatile

Received: March 13, 2024
Revised: May 2, 2024
Accepted: May 16, 2024
Published: May 22, 2024

metabolites are particularly important for quantitative metabolomics. Notably, the loss of volatile metabolites, such as formate, acetate, acetone, and ethanol, holds particular importance due to their roles in cellular metabolic pathways. Formate is an intermediate of cellular one-carbon metabolism;[23] acetate is a precursor of acetyl-CoA, an important agent of the energy transfer cycle;[24] acetone is one of the main products of ketogenesis;[25] and ethanol influences the cellular energy metabolism, being a key precursor of acetaldehyde.[26] In combination, these compounds are important for ethanol degradation, pyruvate metabolism, glucose metabolism, and glyoxylate metabolism. Consequently, misinterpretation of the concentrations of these metabolites may lead to a false understanding of metabolic processes under study. It has become a custom that most scientific publications focus more on the analytical step, whereas the preanalytical step can introduce significant artificial changes into the metabolome in terms of volatile content.[27]

Analysis of volatile organic compounds is often used in scientific studies related to the plant sciences and food industry, where the recovery of volatiles is crucial. In particular, quantification of aroma compounds has been carried out in plant metabolomics to evaluate the product quality after different types of processing.[14,15,28−32] Most of these studies correspond to compounds with a relatively high boiling point and low vapor pressure; however, even for these substances, the extraction recovery is often rather low or variable.[16,33,34] It has been noticed that buffering the solution before the solvent evaporation as well as incomplete sample drying may significantly improve the recovery of volatiles.[33] However, no mechanisms explaining the process of volatile compound retention in dried samples have been proposed. The understanding of mechanisms underlying the drying process for volatile metabolites will allow expanding the metabolite coverage under analysis, making metabolomic discoveries sounder. This work is aimed at the experimental and theoretical study of mechanisms of volatile substance evaporation and/or retention in the residues during the concentration and drying of extract solutions.

EXPERIMENTAL SECTION

Materials. Methanol (MeOH), ethanol, chloroform, and acetone from J.T. Backer (Radnor, USA); 99.9% D_2O from Astrachim (St. Petersburg, Russia); acetic acid, formic acid, glycine, β-alanine, and sodium chloride from Sigma-Aldrich (St. Louis, USA); monosodium phosphate dihydrate and disodium phosphate from Applichem (Darmstadt, Germany); hydrogen chloride from Ecros (St. Petersburg, Russia); sodium hydroxide from Merck (Darmstadt, Germany); and frozen human serum from Sigma-Aldrich (St. Louis, USA) were used as received. H_2O was deionized using an Ultra Clear UV plus water system (SG Water, Hamburg, Germany) to a quality of 18.2 MΩ.

A solution containing 20 mM glycine, β-alanine, acetic acid, formic acid, acetone, and ethanol in deionized H_2O was used in all experiments as a metabolite stock solution. Aqueous phosphate-buffered saline solutions containing NaH_2PO_4, Na_2HPO_4, and NaCl at different concentrations and pH 7.4 were used in the experiments with model solutions. A deuterated buffer solution containing 50 mM sodium phosphates (pH 7.1) and 20 μM sodium 4,4-dimethyl-4-silapentane-1-sulfonate (DSS) as an internal standard was used for NMR measurements and kinetic measurements.

Kinetic Measurements. For kinetic measurements, we added NaCl to concentration of 87 mM (0.5%) and 6 μL of 20 mM stock metabolite solution to 600 μL of 25 mM deuterated buffer solution. We placed tubes with the solution in a rotary vacuum evaporator and removed them at different time intervals. The tubes were then weighed to determine the amount of solvent remaining. Then D_2O was added to the total volume of 600 μL, the solutions were transferred into NMR tubes, and NMR spectra were obtained.

Preparation of Metabolomic Extracts. For the preparation of blood serum metabolomic extract, we followed a standard protocol.[35,36] We added 3÷18 μL of 20 mM stock metabolite solution, 300 μL of cold methanol, and 300 μL of cold chloroform to 300 μL of thawed human blood serum; the mixture was stirred on a shaker at +4 °C (15 min), incubated at −20 °C (30 min), and centrifuged (30 min, 16,100*g*, 4 °C). After centrifugation, the upper water−methanol fraction was collected, vacuum-dried, and then redissolved in the deuterated buffer for NMR analysis. A clean serum extract without additional metabolites was prepared in the same way.

To prepare the metabolomic extract of kidney tissue, we also used a standard methanol/water/chloroform extraction procedure. We added 9.6 mL of cold methanol to a frozen chicken kidney (450 mg). The tissue was homogenized with a rotary homogenizer TissueRuptor II (Qiagen, The Netherlands), and the homogenate was divided into six aliquots of 1600 μL, each containing approximately 75 mg of tissue. Three samples were added to 15 μL of 1 mM stock metabolite solution, and the remaining three served as controls. Then, 800 μL of H_2O and 1600 μL of cold chloroform were added to each sample. The samples were stirred on a shaker at +4 °C (15 min), incubated at −20 °C (30 min), and centrifuged (30 min, 16,100*g*, 4 °C). After that, the upper fractions of each sample were collected, vacuum-dried, and redissolved in the deuterated buffer for NMR analysis. The same treatment of chicken kidney samples was performed using 10 and 20 mM phosphate buffer instead of pure water.

NMR Measurements. ^{1}H NMR measurements were carried out at the Center of Collective Use "Mass spectrometric investigations" SB RAS using an NMR spectrometer AVANCE III HD 700 MHz (Bruker BioSpin, Rheinstetten, Germany). Solutions for NMR measurements were redissolved in 50 mM deuterated phosphate buffer containing 20 μM of DSS as an internal standard and transferred into 5 mm NMR tubes. Spectra were obtained by summing 64 free induction decay signals after 90° pulse exposure. Water signal was presaturated with a low-power selective pulse. The concentrations of metabolites in samples were calculated by integrating their NMR signals relative to the DSS signal.

Theoretical Calculations. Numerical calculations of processes occurring in the solution during vacuum drying were carried out using code written in Matlab version 8.5 R2015a (The MathWorks, Inc., Natick, US) with the use of the Matlab "roots" function to solve polynomial equations.

RESULTS

The majority of experiments in this work were performed for H_2O/MeOH (1:1) model solutions containing different concentrations of phosphate buffer salts (Na_2HPO_4 and NaH_2PO_4), NaCl, and six metabolites: two nonvolatile compounds (glycine and β-alanine) and four volatile metabolites (acetone, ethanol, acetate, and formate). These

https://doi.org/10.1021/acsomega.4c02439
ACS Omega 2024, 9, 24015−24024

Table 1. Portions of Metabolites Remaining in the Samples after Rotary Vacuum Drying[a]

solution	remaining portion (%)					
	formate	acetate	acetone	ethanol	glycine	β-alanine
1	5.3 ± 1.3	0	0	0	102 ± 6	104 ± 6
2	19.0 ± 2.6	0	0	0	99.5 ± 0.8	100.5 ± 1.1
3	80 ± 11	50 ± 15	0	0	100.9 ± 2.4	100 ± 4
4	101 ± 13	74 ± 10	0	0	98.9 ± 2.2	99 ± 3

[a]There are four types of H_2O/MeOH solution: (1) without salts; (2) containing 87 mM NaCl; (3) containing 9.4 mM Na_2HPO_4 and 3.1 mM NaH_2PO_4; and (4) containing 87 mM NaCl, 9.4 mM Na_2HPO_4, and 3.1 mM NaH_2PO_4. The initial concentrations of metabolites were 100 μM. All measurements were carried out in triplicate, and the data are presented as the mean ± standard deviation.

solutions mimic typical metabolomic extracts obtained after the tissue homogenization, protein precipitation, and metabolite extraction. Unless stated otherwise, the initial concentration of each metabolite in solution was 100 μM, and the solution volume was 0.6 mL. The solutions were dried by rotary vacuum evaporation (unless stated otherwise) overnight to complete dryness, the residue was redissolved in deuterated phosphate buffer, and then we measured the concentrations of metabolites in the residue by NMR. Typically, we repeated each experiment three times to assess the variation of the recovery rate. In all measurements, the content of nonvolatile compounds glycine and β-alanine after solvent evaporation remained the same as in the initial solution (Table 1). For that reason, we do not show the levels of these substances in figures, and they served mostly as an additional internal control of possible sample loss.

Influence of Sodium and Phosphate Buffer Salts on the Evaporation of Volatile Metabolites. Vacuum drying of a H_2O/MeOH solution of six metabolites without addition of salts has resulted in the complete evaporation of acetone, ethanol, and acetic acid (their concentrations in the residue were below the detection level) and almost complete evaporation of formic acid (the recovery was only 5% from the initial level). With the addition of 0.5% NaCl (87 mM) to the solution, the portion of formate remaining in the residue increased to 19% from the initial level, whereas acetone, ethanol, and acetate still were not detected. Significant retention of formate and acetate was observed for 12.5 mM phosphate buffer solution (pH 7.4) containing 9.4 mM Na_2HPO_4 and 3.1 mM NaH_2PO_4: the portions of formate and acetate in the residue were 80 and 50%, respectively, of the initial level. The highest retention (100% for formate and 74% for acetate) was achieved with the addition of both phosphates and sodium chloride (Table 1). Acetone and ethanol evaporated completely in all of the solutions. At the same time, we found the presence of residual methanol in all of the samples. The observed level of methanol from sample to sample varied significantly from 0.1 to 0.5 nL.

To test the influence of the salt concentration on volatile metabolite retention in the residue after the vacuum drying, we prepared a stock 1:1 H_2O/MeOH solution containing 3 mM phosphate buffer (pH 7.4) and 2% NaCl (348 mM) and then diluted it with H_2O/MeOH. This way, we obtained nine solutions with the salt concentration varying from 5 to 100% of the stock solution. Six metabolites were added to each solution in the concentration of 100 μM, the solutions were vacuum-dried, and the content of metabolites in the residues was measured. The results of the experiment are presented in Figure 1. Acetone and ethanol evaporated completely, whereas the portion of acetate and formate in the residue remained stable at the level of 0.8−1.0 for most of the samples and started to decrease with the NaCl concentration below 87 mM and phosphate buffer concentration below 0.75 mM.

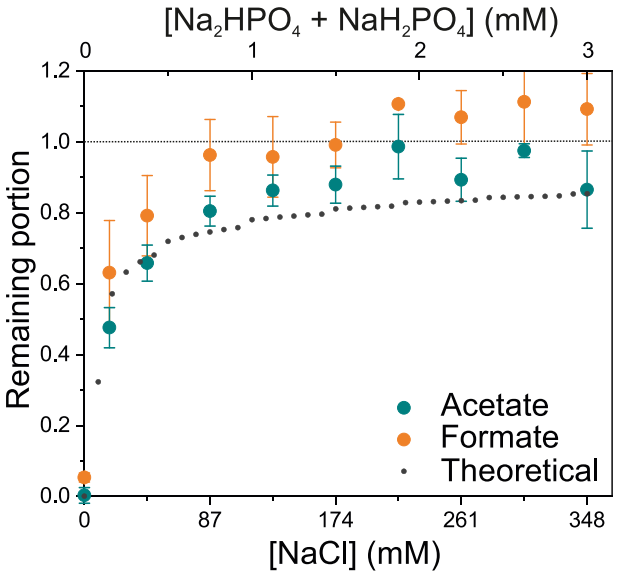

Figure 1. Dependence of acetate and formate recovery after solvent evaporation on the salt concentration. Green circles, acetate; orange circles, formate; and small gray circles, theoretical calculations.

We also tested the influence of the initial metabolite concentration on their retention in the residue (Figure 2). We found that for solutions containing 12.5 mM phosphates and 0.5% NaCl, the content of acetate and formate in the residue did not change with the metabolite concentration varying from 50 to 300 μM (Figure 2A). For solutions with 1 mM phosphates and 0.5% NaCl, the content of acetate started to decrease with the metabolite concentrations above 200 μM, whereas the content of formate did not change (Figure 2B).

Influence of the Initial pH of the Solution on the Evaporation of Volatile Metabolites. For studying the effect of the initial pH of the extract on the retention of volatile metabolites in the residues after the vacuum drying, we used H_2O/MeOH (1:1) solution containing 0.5% NaCl, 12.5 mM phosphates (9.4 mM Na_2HPO_4 and 3.1 mM NaH_2PO_4), and six metabolites in the concentration of 100 μM. We adjusted the initial pH of solution (5.8÷9.0) by adding HCl or NaOH. Again, acetone and ethanol evaporated completely in all types of solution. The dependence of the acetate and formate portions remaining in the residues after vacuum drying is given in Figure 3. Loss of formate is observed with the initial pH below 7.0, and at pH 5.8, the portion of the remaining formate is below 70%. A significant drop for acetate is observed already for pH below 8.0, and at pH 5.8, the portion of the remaining acetate is below 10%.

https://doi.org/10.1021/acsomega.4c02439
ACS Omega 2024, 9, 24015−24024

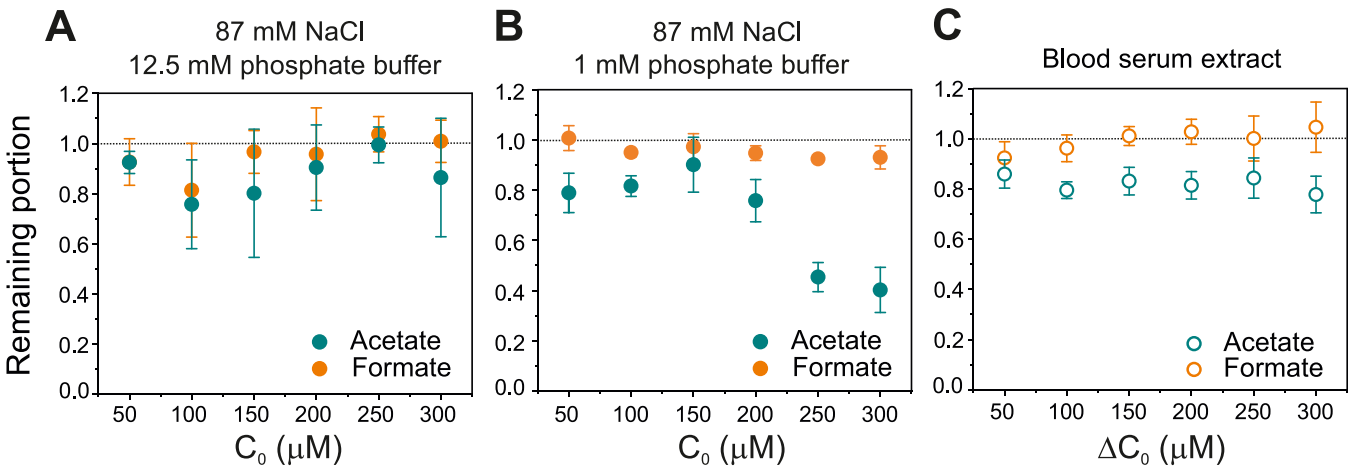

Figure 2. Dependence of acetate and formate recovery after the solvent evaporation on their initial concentration. (A) H_2O/MeOH (1:1) solution containing 12.5 mM phosphates and 0.5% NaCl; (B) H_2O/MeOH (1:1) solution containing 1 mM phosphates and 0.5% NaCl; (C) H_2O/MeOH extract from the human blood serum. ΔC_0 is the concentration of a spiked additive.

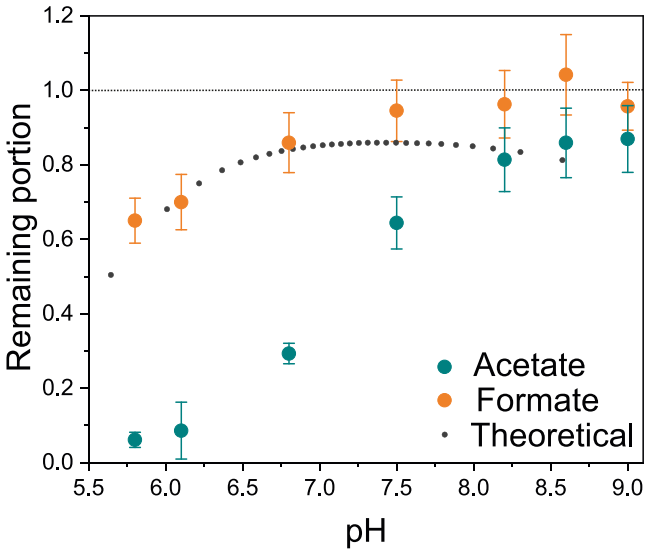

Figure 3. Dependence of acetate and formate recovery after solvent evaporation on the initial pH of solution. Green circles, acetate; orange circles, formate; and small gray circles, theoretical calculations.

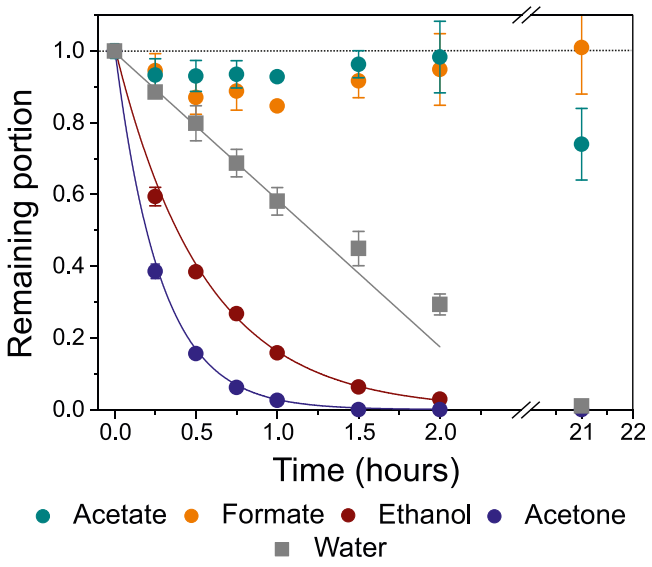

Figure 4. Kinetics of metabolite volatilization during the vacuum evaporation of an aqueous solution containing 25 mM phosphate buffer and 87 mM NaCl. Gray squares, water; green circles, acetate; orange circles, formate; brown circles, ethanol; and blue circles, acetone. The initial metabolite concentrations are 200 μM, and the initial water volume is 600 μL. Solid lines show linear (for water) and exponential (for ethanol and acetone) fits.

Kinetics of Metabolite Evaporation. The kinetics of metabolite volatilization was measured for six metabolites (200 μM) dissolved in 25 mM deuterated phosphate buffer (without methanol). We placed tubes with the solution into the rotary vacuum evaporator and removed them (in triplicate) after the different time intervals. The amount of water in the tubes was determined by tube weighting. We transferred the solutions into NMR tubes, added D_2O to the total volume of 600 μL, and obtained the NMR spectra. Figure 4 shows that the content of water in the tube decreases linearly, whereas the content of nondissociating compounds acetone and ethanol decreases exponentially during the drying. The levels of formate and acetate remained stable during almost the whole experiment, and an approximately 20−30% loss of acetate was observed only at the end of evaporation.

Evaporation of Volatile Metabolites from Biological Extracts. To compare the results obtained for model solutions of six metabolites with real metabolomic extracts, we carried out experiments with human blood serum. We added volatile metabolites (acetone, ethanol, acetate, and formate) to the serum samples in the concentrations varying from 0 to 300 μM and then performed the procedure of the sample preparation. After vacuum evaporation, we did not detect acetone and ethanol in the samples, whereas acetate and formate were found in all extracts. Extracts without spiked additives also contained some native levels of acetate and formate. To calculate the portion of acetate and formate remaining in the extract, we subtracted the native concentration measured in the samples from the total concentration measured in the samples with spiked metabolites. The results are presented in Figure 2C. We found that almost 100% of additional formate and about 80% of additional acetate remained in the residue after the vacuum drying; these amounts do not depend on the initial concentration of metabolites. These results are in good

https://doi.org/10.1021/acsomega.4c02439
ACS Omega 2024, 9, 24015−24024

agreement with the data obtained for the model solutions with sodium and phosphate buffer salts.

A similar experiment was carried out for metabolomic extracts from chicken kidney. Measurements were performed in triplicate for the extact without addition of metabolites and for the extract with the same six compounds added at a concentration of 200 nmol/g of kidney tissue before extracting and drying the sample. We found that, in this case, the retention of volatile acids in solution during drying is significantly lower than in the case of serum extract: formate recovery was only 64 ± 3%, and acetate recovery was 38 ± 7%. However, the addition of buffer salts during extraction significantly increased the degree of recovery: the use of 10 mM phosphate buffer instead of pure water increased the recovery of formate to 93 ± 5% and that of acetate to 68 ± 8%. The use of 20 mM buffer resulted in the almost complete recovery of both acids: 95 ± 6% for formate and 78 ± 8% for acetate.

Control Experiments. To check the generality of the effects observed, we performed two control experiments. In the first experiment, we replaced the oil-sealed rotary vane pump used in all previous experiments for vacuum drying (pressure 0.01 mbar) with a membrane pump (pressure 10 mbar). In the second experiment, we used a sample lyophilization technique instead of vacuum drying. The measurements were performed for H_2O/MeOH (1:1) solutions containing 0.5% NaCl, 12.5 mM phosphates (pH 7.4), and six metabolites with a concentration of 100 μM. The general outcome of both experiments was essentially the same as in the case of vacuum drying with the use of the rotary vane pump: acetone and ethanol evaporated completely, whereas significant portions of acetate and formate remained in the residues. In particular, the quantities of formate and acetate were approximately 100 and 70%, respectively, in the case of vacuum drying with the membrane pump and about 80 and 40% in the case of lyophilization. The results of the control experiments indicate that the observed effects, in general, do not depend on the method of sample concentration and on the pump type. Most likely, drying of the extracts under nitrogen flow will give the same result.

Modeling the Evaporation of Dissociating Volatile Metabolites under the Sample Vacuum Drying. To understand better the mechanisms of volatile metabolite evaporation or retention in the dried extract, we performed model calculations of the processes occurring during the sample vacuum drying. Several processes occur in the system that need to be taken into account: evaporation of solvent molecules leading to changes in the solution volume and increase of all concentrations; evaporation of volatile metabolites; loss of solubility and thus precipitation of NaCl and buffer salts; and trapping volatile metabolites in the solid salt matrix.

Let us consider an aqueous solution containing salts Na_2HPO_4, NaH_2PO_4, and NaCl and a dissociating acid RH. In the initial solution, salts dissociate completely, yielding ions HPO_4^{2-}, $H_2PO_4^-$, Na^+, H^+, and Cl^-. These ions are in equilibrium:

$$H_2PO_4^- \rightleftarrows HPO_4^{2-} + H^+ \quad (1)$$

Depending on the pH of solution, the acid RH can exist in either the associated (RH) or dissociated (R^-) state; it can also form the RNa salt:

$$RH \leftrightarrows R^- + H^+ \quad (2)$$

$$RNa \rightleftarrows R^- + Na^+ \quad (3)$$

We assume that the solution evaporation and the solute precipitation under exceeding the solubility limits proceed much slower than reactions 1−3; i.e., at any instance of time, the concentrations of ions are in equilibrium. Therefore, we can use the so-called pre-equilibrium approximation (PEA; also called the partial equilibrium approximation or fast-equilibrium approximation).[37]

The equilibrium constant for reaction 1 is equal to $k_{eq} = 6.2 \times 10^{-8}$ M ($pK_a = 7.2$);[38] for reaction 2, $k_H = 1.8 \times 10^{-5}$ M ($pK_a = 4.75$)[39] in the case of acetic acid and $k_H = 1.8 \times 10^{-4}$ M ($pK_a = 3.75$)[40] in the case of formic acid. For model calculations, we used the value for acetic acid, $k_H = 1.8 \times 10^{-5}$ M. The equilibrium constant for reaction 3 of sodium acetate is $k_{Na} = 25.1$ M ($pK_{Na} = -1.4$).[41]

Thus, the concentrations $[R^-]$, [RH], and [RNa] can be expressed as

$$[R^-] = \frac{[R]}{1 + \frac{[H^+]}{k_H} + \frac{[Na^+]}{k_{Na}}} \quad (4)$$

$$[RH] = \frac{[R]}{1 + \frac{[H^+]}{k_H} + \frac{[Na^+]}{k_{Na}}} \cdot \frac{[H^+]}{k_H} = \frac{[R]}{1 + \frac{k_H}{[H^+]} + \frac{k_H \cdot [Na^+]}{k_{Na} \cdot [H^+]}} \quad (5)$$

$$[RNa] = \frac{[R]}{1 + \frac{[H^+]}{k_H} + \frac{[Na^+]}{k_{Na}}} \cdot \frac{[Na^+]}{k_{Na}} \quad (6)$$

Here, $[R]$ is the total concentration of compounds containing group R: $[R] = [R^-] + [RH] + [RNa]$. Substituting the values of the equilibrium constants k_H and k_{Na} into eqs 4−6 shows that in the initial solution, the acid is present almost entirely in the dissociated state R^-: for pH 7.4, only 0.04% and 0.35% of the substance are present in the associated forms RH and RNa, respectively.

Using equations for the conservations of the total charge, phosphorus, Na^+, and Cl^-, one can write an equation determining the pH value of solution:

$$[NaH_2PO_4] + 2 \cdot [Na_2HPO_4] + [H^+] = P + \frac{k_{eq} P}{[H^+] + k_{eq}} + \frac{[R]}{1 + \frac{[H^+]}{k_H} + \frac{[Na^+]}{k_{Na}}} \quad (7)$$

where $P = [Na_2HPO_4] + [NaH_2PO_4]$ and $[Na^+] = [NaCl] + [NaH_2PO_4] + 2[Na_2HPO_4]$. Before the solubility limit was reached, the concentrations of sodium salts were calculated as the ratios of the amount of salt (in moles) to the current volume. After this, the salt concentration was considered constant and equal to the maximum possible concentration. The last term in eq 7 describes the effect of RH on solution acidity. At the beginning of evaporation, it is much lower than the two other terms in the right part of the equation (because $P \gg [R]$). However, under solvent evaporation and salt precipitation, the $[R]$ value may become comparable to the P value. For that reason, we calculated the current $[H^+]$ values using eq 7 with all terms. Equation 7 was recast into a cubic equation for $[H^+]$, which we solved using the "roots" procedure in Matlab.

https://doi.org/10.1021/acsomega.4c02439
ACS Omega 2024, 9, 24015−24024

The pH value remains constant during almost the whole time of the solution evaporation and starts to change only when the buffer salts reach the solubility limits (Figure 5). It is important to note that in the pH calculations, we did not take into account the ionic strength of the solution, which changes quite strongly when the solvent evaporates. Therefore, the calculated pH values can differ from the experimental values. However, in this work, we are trying to get a qualitative agreement between the theoretical calculations and experimental data rather than achieve a perfect fit, so we neglected the ionic strength influence.

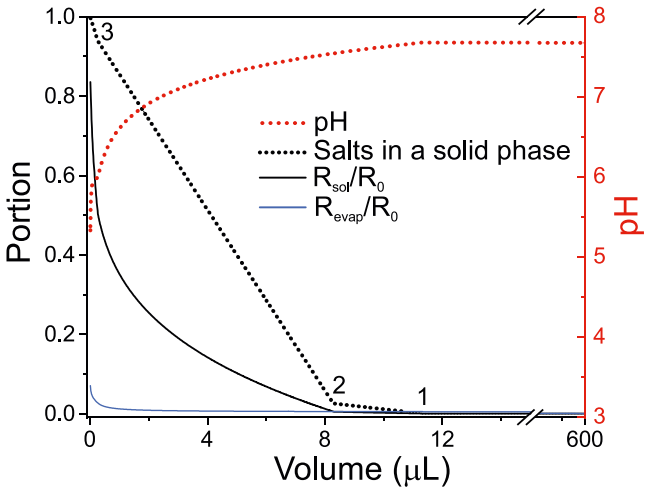

Figure 5. Calculated kinetics of processes occurring during solvent evaporation. Red dotted line, pH changes; black dotted line, formation of the solid salt matrix; bold black line, trapping of the acid in the solid matrix; and thin gray line, evaporation of acid RH. Point 1 indicates the beginning of Na_2HPO_4 precipitation, point 2 indicates the beginning of NaCl precipitation, and point 3 indicates the beginning of NaH_2PO_4 precipitation.

The evaporation of volatile metabolites can occur only for those in the associated form RH. According to Henry's law, the rate of RH evaporation λ_{evap} is proportional to its molar concentration:

$$\lambda_{evap} = \alpha[\mathrm{RH}] \tag{8}$$

where α is the constant depending on the vapor pressure. Taking into account that the vapor pressures at 20 °C for water (17.4 mmHg), formic acid (33.1 mmHg), and acetic acid (11.7 mmHg) are of the same order of magnitude,[42] in model calculations, we assumed the same value of α for both solvent and RH. In the initial solution, 100% water and only 0.04% acid are present in the volatile associated state; therefore, at the initial stage, the relative rate of the water evaporation is 2500 times higher than that of the acid. In other words, the total amount of compounds containing group R in solution practically does not change until almost all of the solvent has evaporated. When the solution volume becomes as small as a few tens of microliter, the concentrations of buffer salts and NaCl increase dramatically and approach the solubility limit, and salts start to precipitate. The limits of solubility are 360 g/L (6.3 M) for NaCl, 870 g/L (10.6 M) for NaH_2PO_4, and 80 g/L (0.5 M) for Na_2HPO_4.[43] Therefore, Na_2HPO_4 is the first compound that starts to precipitate. This will cause the pH of solution to decrease (Figure 5) and the molar concentration of the associated form RH to increase. Correspondingly, the rate of RH evaporation also increases. It should be noted that, at this stage, the solubility limit for acid salt RNa is not yet reached (750 g/L for sodium acetate and 810 g/L for sodium formate),[43] and the RNa itself cannot form precipitating crystals. At the same time, R-containing molecules can be captured in the solid matrix of precipitating salts;[44,45] these molecules will remain in the residue until the end of evaporation. Therefore, the portion of R-containing compounds in the residue is determined by the competition between two processes: the solute volatilization in the RH form and the metabolite trapping in the solid matrix formed by sodium chloride and phosphate salts.

The rate of the metabolite trapping λ_{tr} in the salt matrix is proportional to the rate of the solid phase formation λ_{sol} and to the concentration of compounds containing group R:

$$\lambda_{tr} = \eta \cdot \lambda_{sol} \cdot [R] \tag{9}$$

η is the constant characterizing the capture of a metabolite in the solid salt matrix. Let us denote the total number of moles (not the concentration!) of compounds containing the functional group R in solution as simply R (RH, RNa, and R^-), the number of moles of evaporated RH as RH_{evap}, and the number of moles of compounds trapped in the solid matrix as R_{sol},

$$R + \mathrm{RH}_{evap} + R_{sol} = \mathrm{const} \tag{10}$$

or

$$\frac{dR}{dt} + \frac{d\mathrm{RH}_{evap}}{dt} + \frac{dR_{sol}}{dt} = 0 \tag{11}$$

because

$$\frac{d\mathrm{RH}_{evap}}{dt} = \lambda_{evap} = \alpha[\mathrm{RH}] \tag{12}$$

and

$$\frac{dR_{sol}}{dt} = \lambda_{tr} = \eta \cdot \lambda_{sol} \cdot [R] \tag{13}$$

eq 11 can be rewritten as

$$\frac{dR}{dt} + \frac{\alpha R}{V} f + \eta \cdot \lambda_{sol} \cdot \frac{R}{V} = 0 \tag{14}$$

where

$$f = \frac{1}{1 + \frac{k_H}{[H^+]} + \frac{k_{H'}[Na^+]}{k_{Na'}[H^+]}} \tag{15}$$

f is the parameter depending on pH and pNa, and V is the current volume of solution. We assume that V decreases linearly with time,

$$V(t) = V_0 - \alpha \cdot t \tag{16}$$

and

$$\frac{dR}{dt} = -\alpha \cdot \frac{dR}{dV} \tag{17}$$

Now, eq 14 takes the form

$$\frac{dR}{dV} = \frac{R}{V} \cdot f + \frac{\eta}{\alpha} \lambda_{sol} \frac{R}{V} \tag{18}$$

We replace eq 18 with an implicit difference scheme:

https://doi.org/10.1021/acsomega.4c02439
ACS Omega 2024, 9, 24015−24024

$$\frac{R(V) - R(V - \Delta V)}{\Delta V} = \frac{R(V - \Delta V)}{V} \cdot \left(f + \frac{\eta}{\alpha} \cdot \lambda_{sol}\right) \quad (19)$$

Finally, the current values of R (in solution), RH_{evap} (evaporated), and R_{sol} (trapped in solid matrix) after the evaporation of ΔV of the solvent volume can be calculated as

$$R(V - \Delta V) = \frac{R(V)}{1 + \frac{\Delta V}{V}\left(f + \frac{\eta}{\alpha} \cdot \lambda_{sol}\right)} \quad (20)$$

$$RH_{evap}(V - \Delta V) = RH_{evap}(V) + R(V) \cdot f \cdot \frac{\Delta V}{V} \quad (21)$$

$$R_{sol}(V - \Delta V) = R_{sol}(V) + R(V) \cdot \frac{\eta}{\alpha} \cdot \lambda_{sol} \cdot \frac{\Delta V}{V} \quad (22)$$

We performed the calculations of the evaporation kinetics in the following way. The starting conditions were as follows: V = 600 μL, [NaCl] = 87 mM, [Na_2HPO_4] = 9.4 mM, [NaH_2PO_4] = 3.1 mM, and [RH] = 0.1 mM. The whole range of the solution volumes (from 600 to 0 μL) was divided into two regions: in the initial region (from 600 to 50 μL), the calculations were performed with the step of 6 μL, and in the final region (from 50 μL to zero), they were performed with the step of 0.006 μL. First, we found the values of H^+ concentration for each point according to eq 7 and calculated the f values (eq 15). Then the current values of R, RH_{evap}, and R_{sol} were calculated. The only variable parameter was the ratio η/α, which determines the competition between the RH volatilization and R trapping in the solid salt matrix. Figure S2 shows the dependence of R_{sol}/R_0 on η/α, where R_0 is the initial molar content of a metabolite. A good agreement between the calculations and experimental data was achieved with η/α = 0.03 (Figures 1 and 3). Figure 5 shows the calculated kinetics of the pH change, acid evaporation, and acid entrapment in the solid matrix under drying of a solution containing both NaCl and buffer salts, and Figure S3 demonstrates the same events in a solution with only NaCl and only buffer salts.

DISCUSSION

In this work, we studied the evaporation of volatile compounds with low boiling points and high vapor pressures from metabolomic extracts during vacuum drying. The results obtained show that the main factor determining the retention of volatile compounds in the residue after solvent evaporation is their ability to dissociate in solution. Nondissociating compounds such as acetone and ethanol volatilize completely or almost completely independently of the method of sample concentration (evaporation or lyophilization), type of pump, and pH of solution. Methanol was present in the initial solution in the volume of 300 μL, and after the vacuum evaporation, the amount of MeOH in the residue was 0.1−0.5 nL, indicating only 10^{-6} recovery of this substance. Most likely, the presence of volatile nondissociating compounds like ethanol, methanol, or acetone in dried extracts from biological tissues[17−22] should be attributed to their trapping in the solid salt matrix at the last stage of evaporation. Apparently, the measured concentrations of these compounds are much lower than those in the initial solutions. Taking into account the extremely low recovery, the mere detection of ethanol or acetone in dried extracts indicates a very high level of these metabolites in the tissue under study. Therefore, correct measurements of nondissociating volatile compounds in biological samples should be made without concentrating the extract by using raw biological fluids (such as blood serum or urine) or by application of MAS NMR for raw tissue samples.

An acid can leave the solution only in the associated form RH, and as long as it is present mostly in the dissociated form R^-, it remains in the solution. However, in the absence of significant amounts of buffer salts, the presence of acids can decrease the pH of the solution, causing the equilibrium in eq 2 to shift to the left side. The concentration of the associated form RH will significantly increase as well as the rate of RH evaporation. Eventually, without buffer salts, almost all of the acid will evaporate. Therefore, buffer salts have two important functions for the acid retention: they maintain the pH of the solution at a sufficiently high level, and, under precipitation, they form a solid matrix for metabolite trapping. Figure 3 shows that maintaining high pH plays a crucial role in the acid retention: the loss of acetate from the solution with the initial pH 6 is much higher than the loss of formate, although the vapor pressure for formate is 3-fold higher than that for acetate, and the boiling point is lower. The observed difference between formate and acetate should be attributed to the higher pK_a value of acetic acid, so the left shift in eq 2 for acetic acid occurs earlier.

The presence of NaCl does not help to maintain the high pH of the solution, and without buffers, volatile acids readily evaporate from the solution (Table 1, Figure S3). However, in buffer solutions, high concentrations of NaCl assist the formation of solid matrix for metabolite trapping and improve the retention of volatile dissociating metabolites in the residue (Table 1).

Figure 5 illustrates the sequence of events occurring in the solution during the evaporation. Initially, there is no significant change until the solution volume becomes as low as 11 μL (1.83% of the initial 600 μL): the pH of the solution remains at the initial level due to phosphate buffer salts, and the dissolved acid remains in the solution almost completely in the dissociated state R^-. When the solution volume is less than 11 μL, one of the buffer salts, disodium Na_2HPO_4, begins to precipitate, forming a solid matrix. The pH value of the solution starts to decrease, and a portion of the RH becomes trapped in the solid matrix. With a solution volume of 8 μL, the solubility limit of NaCl is reached. The precipitation of NaCl does not influence the pH of the solution but significantly accelerates the solid matrix formation and RH capture in this matrix. The most important events occur when the solution volume becomes less than 0.5 μL. At that time, the second buffer salt, monosodium NaH_2PO_4, begins to precipitate, and the acid concentration becomes so high that the pH of the solution quickly goes down and approaches the pK_a value of the acid. The molar concentration of the associated form RH strongly increases, and the evaporation of the acid occurs mostly during the evaporation of the very last drop of solution.

Measurements of formate and acetate retention in the residue after evaporation of serum extract show that human blood contains sufficient quantities of buffers and NaCl to retain virtually all formate and about 80% acetate. For living organisms, it is essential to maintain a neutral blood pH of 7.4. This is provided by several buffer systems including chemical buffers like carbonates and phosphates, proteins, and red blood cells.[46] Blood serum normally contains about 0.9% NaCl, 25 mM carbonate−bicarbonate components, and 1.2 mM phosphate salts.[47,48] Because there is no crucial difference between the buffer capacity of these systems and the

https://doi.org/10.1021/acsomega.4c02439
ACS Omega 2024, 9, 24015−24024

solubilities of sodium bicarbonate and disodium phosphate are fairly close, we suppose that our model describes well the processes occurring during the drying of the blood serum extract. Very likely, many other animal tissues also contain sufficient amounts of buffers. However, under certain conditions (for example, accumulation of lactate in muscles under intensive exercises), the strength of the internal tissue buffers could not be sufficient to maintain the high pH. This may cause the increase in the volatile acid loss during the evaporation. Measurements performed for chicken kidneys illustrate this case. The measured level of lactate in chicken kidney (24 μmol/gram) was much higher than that in human serum (1.8 mM), and the recovery of acetate and formate after drying kidney extracts was significantly lower. This experiment also demonstrates the advantage of using a buffer solution instead of pure water during extraction: in this case, the recovery of volatile acids significantly increases. Figure 2B also shows that a high acid concentration and insufficient buffer capacity lead to poor acid recovery under solution evaporation.

For plants and foods, the situation is most probably different. The content of salts in many plant tissues is much lower than that in animal tissues. For that reason, the loss of volatile metabolites during drying of plant material is rather high even for compounds with relatively low vapor pressure.[33,34]

There are several ways to improve the retention of acids in the residue and avoid errors in volatile acid content measurements. The simplest way is incomplete sample drying: our calculations and experimental findings indicate that acid evaporation occurs at the very last stage of the drying, and leaving several microliters of the solvent in a sample should prevent acid evaporation. However, for a batch metabolomics experiment containing a large number of samples, the condition of a similar residual volume for all samples may be difficult to achieve: evaporation for samples in different vials may occur at different speeds. Acid retention can also be improved by increasing the pH of the extract before evaporation, by adding buffer salts to maintain high pH, or by adding NaCl to the extract. However, high concentrations of NaCl in a sample can create problems at the analytical stage of the measurements by decreasing the Q factor and thus the sensitivity (Figure S2) of an NMR probe (in the case of NMR-based metabolomics) or contamination of a mass spectrometer (in the case of MS-based metabolomics). By our estimations, physiological 0.9% NaCl concentrations are close to the optimal value. Our recommendations are in a good agreement with previous results,[33] where incomplete drying of the sample and buffering the solution significantly improved the recovery of salicylic acid under evaporation of extracts.

CONCLUSIONS

The results obtained in the present work indicate that solvent evaporation from metabolomic extracts leads to the unavoidable loss of nondissociating volatile metabolites with low boiling points and high vapor pressure. The correct measurements of such compounds can be performed only for nonconcentrated extracts or for biological fluids without preliminary treatment. The retention of dissociating volatile compounds (acids in particular) during the evaporation depends on the presence of buffer components and salts, which maintain the high pH of the solution and form a solid matrix for metabolite trapping at the final stage of evaporation. Typical metabolomic extracts from animal tissues contain sufficient amounts of NaCl and buffer salts to retain virtually all formate and most of acetate; the retention of volatile acids can be improved either by adding buffer salts to maintain high pH or by incomplete sample drying.

ASSOCIATED CONTENT

Supporting Information

The Supporting Information is available free of charge at https://pubs.acs.org/doi/10.1021/acsomega.4c02439.

Figure S1: calculated dependence of the recovery of acid RH after the solution drying on the η/α ratio; Figure S2: decay of the DSS NMR signal in the presence of NaCl at various concentrations; Figure S3: calculated kinetics of processes occurring during the solvent evaporation; and Appendix: Matlab code used to simulate the processes occurring in solution during vacuum drying (PDF)

AUTHOR INFORMATION

Corresponding Author

Yuri P. Tsentalovich − *International Tomography Center Siberian Branch of Russian Academy of Sciences, Novosibirsk 630090, Russia;* orcid.org/0000-0002-1380-3000; Email: yura@tomo.nsc.ru

Authors

Nataliya A. Osik − *International Tomography Center Siberian Branch of Russian Academy of Sciences, Novosibirsk 630090, Russia;* orcid.org/0000-0002-9338-1409

Nikita N. Lukzen − *International Tomography Center Siberian Branch of Russian Academy of Sciences, Novosibirsk 630090, Russia; Novosibirsk State University, Novosibirsk 630090, Russia*

Vadim V. Yanshole − *International Tomography Center Siberian Branch of Russian Academy of Sciences, Novosibirsk 630090, Russia; Novosibirsk State University, Novosibirsk 630090, Russia;* orcid.org/0000-0003-1512-3049

Complete contact information is available at: https://pubs.acs.org/10.1021/acsomega.4c02439

Author Contributions

The manuscript was written through contributions of all authors. Conceptualization, Y.P.T., V.V.Y., and N.A.O.; methodology, formal analysis, data curation, N.A.O; theoretical calculations N.N.L.; writing − original draft preparation, Y.P.T. and N.A.O.; writing − review and editing, Y.P.T., N.A.O., V.V.Y., N.N.L.; supervision, Y.P.T. All authors have read and agreed to the published version of the manuscript.

Notes

The authors declare no competing financial interest.

ACKNOWLEDGMENTS

This work was financially supported by the Russian Science Foundation, Project 23-25-00462. We thank the Ministry of Science and Higher Education of the RF for the access to NMR equipment.

REFERENCES

(1) Vuckovic, D. Chapter 4 - Sample Preparation in Global Metabolomics of Biological Fluids and Tissues. In *Proteomic and Metabolomic Approaches to Biomarker Discovery* (2 Edition); Issaq, H. J., Veenstra, T. D., Eds.; Academic Press: lBoston, 2020; pp 53−83. DOI: 10.1016/B978-0-12-818607-7.00004-9.

(2) Mal, T. K.; Tian, Y.; Patterson, A. D. Sample Preparation and Data Analysis for NMR-Based Metabolomics. *Methods Mol. Biol.* **2021**, *2194*, 301−313.
(3) Snytnikova, O. A.; Khlichkina, A. A.; Sagdeev, R. Z.; Tsentalovich, Y. P. Evaluation of Sample Preparation Protocols for Quantitative NMR-Based Metabolomics. *Metabolomics* **2019**, *15* (6), 84 DOI: 10.1007/s11306-019-1545-y.
(4) Fomenko, M. V.; Yanshole, L. V.; Tsentalovich, Y. P. Stability of Metabolomic Content during Sample Preparation: Blood and Brain Tissues. *Metabolites* **2022**, *12* (9), 811.
(5) Wishart, D. S. NMR Metabolomics: A Look Ahead. *J. Magn. Reson.* **2019**, *306*, 155−161.
(6) Nagana Gowda, G. A.; Raftery, D. Can NMR Solve Some Significant Challenges in Metabolomics? *J. Magn. Reson.* **2015**, *260*, 144−160.
(7) Silva, C. L.; Perestrelo, R.; Capelinha, F.; Tomás, H.; Câmara, J. S. An Integrative Approach Based on GC−qMS and NMR Metabolomics Data as a Comprehensive Strategy to Search Potential Breast Cancer Biomarkers. *Metabolomics* **2021**, *17* (8), 72.
(8) Zeki, Ö. C.; Eylem, C. C.; Reçber, T.; Kır, S.; Nemutlu, E. Integration of GC−MS and LC−MS for Untargeted Metabolomics Profiling. *J. Pharm. Biomed. Anal.* **2020**, *190*, No. 113509.
(9) Maier, T. V.; Schmitt-Kopplin, P. Capillary Electrophoresis in Metabolomics. *Methods Mol. Biol.* **2016**, *1483*, 437−470.
(10) Lokhov, P. G.; Balashova, E. E.; Trifonova, O. P.; Maslov, D. L.; Archakov, A. I. Ten Years of the Russian Metabolomics: History of Development and Achievements. *Biomed. khimiya* **2020**, *66* (4), 279−293.
(11) Petrova, I.; Xu, S.; Joesten, W. C.; Ni, S.; Kennedy, M. A. Influence of Drying Method on NMR-Based Metabolic Profiling of Human Cell Lines. *Metabolites* **2019**, *9* (11), 256.
(12) Liebeke, M.; Puskás, E. Drying Enhances Signal Intensities for Global GC−MS Metabolomics. *Metabolites* **2019**, *9* (4), 68.
(13) Oikawa, A.; Otsuka, T.; Jikumaru, Y.; Yamaguchi, S.; Matsuda, F.; Nakabayashi, R.; Takashina, T.; Isuzugawa, K.; Saito, K.; Shiratake, K. Effects of Freeze-Drying of Samples on Metabolite Levels in Metabolome Analyses. *J. Sep. Sci.* **2011**, *34* (24), 3561−3567.
(14) Venskutonis, P. R. Effect of Drying on the Volatile Constituents of Thyme (*Thymus Vulgaris* L.) and Sage (*Salvia Officinalis* L.). *Food Chem.* **1997**, *59* (2), 219−227.
(15) D'Auria, M.; Racioppi, R. The Effect of Drying of the Composition of Volatile Organic Compounds in Rosmarinus Officinalis, Laurus Nobilis, Salvia Officinalis and Thymus Serpyllum. A HS-SPME-GC-MS Study. *Journal of Essential Oil Bearing Plants* **2015**, *18* (5), 1209−1223.
(16) Verpoorte, R.; Choi, Y. H.; Mustafa, N. R.; Kim, H. K. Metabolomics: Back to Basics. *Phytochemistry Reviews* **2008**, *7* (3), 525−537.
(17) Lin, Y.; Ma, C.; Bezabeh, T.; Wang, Z.; Liang, J.; Huang, Y.; Zhao, J.; Liu, X.; Ye, W.; Tang, W.; Ouyang, T.; Wu, R. 1 H NMR-Based Metabolomics Reveal Overlapping Discriminatory Metabolites and Metabolic Pathway Disturbances between Colorectal Tumor Tissues and Fecal Samples. *Int. J. Cancer* **2019**, *145* (6), 1679−1689.
(18) Zheng, H.; Dong, B.; Ning, J.; Shao, X.; Zhao, L.; Jiang, Q.; Ji, H.; Cai, A.; Xue, W.; Gao, H. NMR-Based Metabolomics Analysis Identifies Discriminatory Metabolic Disturbances in Tissue and Biofluid Samples for Progressive Prostate Cancer. *Clin. Chim. Acta* **2020**, *501*, 241−251.
(19) Sylvestre, D. A.; Otoki, Y.; Metherel, A. H.; Bazinet, R. P.; Slupsky, C. M.; Taha, A. Y. Effects of Hypercapnia/Ischemia and Dissection on the Rat Brain Metabolome. *Neurochem. Int.* **2022**, *156*, No. 105294.
(20) Palma, M.; Scanlon, T.; Kilminster, T.; Milton, J.; Oldham, C.; Greeff, J.; Matzapetakis, M.; Almeida, A. M. The Hepatic and Skeletal Muscle Ovine Metabolomes as Affected by Weight Loss: A Study in Three Sheep Breeds Using NMR-Metabolomics. *Sci. Rep* **2016**, *6* (1), 39120.
(21) Nicholas, P. C.; Kim, D.; Crews, F. T.; Macdonald, J. M. 1H NMR-Based Metabolomic Analysis of Liver, Serum, and Brain Following Ethanol Administration in Rats. *Chem. Res. Toxicol.* **2008**, *21* (2), 408−420.
(22) Shekhovtsov, S. V.; Bulakhova, N. A.; Tsentalovich, Y. P.; Zelentsova, E. A.; Meshcheryakova, E. N.; Poluboyarova, T. V.; Berman, D. I. Metabolomic Analysis Reveals That the Moor Frog Rana Arvalis Uses Both Glucose and Glycerol as Cryoprotectants. *Animals* **2022**, *12* (10), 1286.
(23) Pietzke, M.; Meiser, J.; Vazquez, A. Formate Metabolism in Health and Disease. *Mol. Metab* **2020**, *33*, 23−37.
(24) Bose, S.; Ramesh, V.; Locasale, J. W. Acetate Metabolism in Physiology, Cancer, and Beyond. *Trends Cell Biol.* **2019**, *29* (9), 695−703.
(25) Owen, O. E.; Trapp, V. E.; Skutches, C. L.; Mozzoli, M. A.; Hoeldtke, R. D.; Boden, G.; Reichard, G. A., Jr. Acetone Metabolism During Diabetic Ketoacidosis. *Diabetes* **1982**, *31* (3), 242−248.
(26) Wilson, D. F.; Matschinsky, F. M. Ethanol Metabolism: The Good, the Bad, and the Ugly. *Med. Hypotheses* **2020**, *140*, No. 109638.
(27) Tkachev, A. V. Problems of the Qualitative and Quantitative Analysis of Plant Volatiles. *Russ J. Bioorg Chem.* **2018**, *44* (7), 813−833.
(28) Juhari, N. H.; Martens, H. J.; Petersen, M. A. Changes in Physicochemical Properties and Volatile Compounds of Roselle (Hibiscus Sabdariffa L.) Calyx during Different Drying Methods. *Molecules* **2021**, *26* (20), 6260.
(29) Nunes, J. C.; Lago, M. G.; Castelo-Branco, V. N.; Oliveira, F. R.; Torres, A. G.; Perrone, D.; Monteiro, M. Effect of Drying Method on Volatile Compounds, Phenolic Profile and Antioxidant Capacity of Guava Powders. *Food Chem.* **2016**, *197* (Pt A), 881−890.
(30) Nöfer, J.; Lech, K.; Figiel, A.; Szumny, A.; Carbonell-Barrachina, Á. A. The Influence of Drying Method on Volatile Composition and Sensory Profile of *Boletus Edulis*. *J. Food Quality* **2018**, *2018*, No. e2158482.
(31) Xia, J.; Guo, Z.; Fang, S.; Gu, J.; Liang, X. Effect of Drying Methods on Volatile Compounds of Burdock (Arctium Lappa L.) Root Tea as Revealed by Gas Chromatography Mass Spectrometry-Based Metabolomics. *Foods* **2021**, *10* (4), 868.
(32) Xie, H.; Zhao, R.; Liu, C.; Wu, Y.; Duan, X.; Hu, J.; Yang, F.; Wang, H. Dynamic Changes in Volatile Flavor Compounds, Amino Acids, Organic Acids, and Soluble Sugars in Lemon Juice Vesicles during Freeze-Drying and Hot-Air Drying. *Foods* **2022**, *11* (18), 2862.
(33) Verberne, M. C.; Brouwer, N.; Delbianco, F.; Linthorst, H. J. M.; Bol, J. F.; Verpoorte, R. Method for the Extraction of the Volatile Compound Salicylic Acid from Tobacco Leaf Material. *Phytochem Anal* **2002**, *13* (1), 45−50.
(34) Villas-Bôas, S. G.; Højer-Pedersen, J.; Akesson, M.; Smedsgaard, J.; Nielsen, J. Global Metabolite Analysis of Yeast: Evaluation of Sample Preparation Methods. *Yeast* **2005**, *22* (14), 1155−1169.
(35) Zelentsova, E. A.; Yanshole, L. V.; Melnikov, A. D.; Kudryavtsev, I. S.; Novoselov, V. P.; Tsentalovich, Y. P. Post-Mortem Changes in Metabolomic Profiles of Human Serum, Aqueous Humor and Vitreous Humor. *Metabolomics* **2020**, *16* (7), 80.
(36) Lin, C. Y.; Wu, H.; Tjeerdema, R. S.; Viant, M. R. Evaluation of Metabolite Extraction Strategies from Tissue Samples Using NMR Metabolomics. *Metabolomics* **2007**, *3* (1), 55−67.
(37) Turányi, T.; Tomlin, A. S. Reaction Kinetics Basics. In *Analysis of Kinetic Reaction Mechanisms*; Turányi, T., Tomlin, A. S., Eds.; Springer: Berlin, Heidelberg, 2014; pp 5−37. DOI: 10.1007/978-3-662-44562-4_2.
(38) Bates, R. G.; Acree, S. F. pH values of certain phosphate-chloride mixtures, and the second dissociation constant of phosphoric acid from 0 degrees to 60 degrees C. *J. Res. Natl. Bur. Stand.* **1943**, *30* (30), 129−155.
(39) Partanen, J. I.; Covington, A. K. Determination of stoichiometric dissociation constants of acetic acid in aqueous solutions containing acetic acid, sodium acetate, and sodium chloride at (0 to 60)° C. *Journal of Chemical & Engineering Data 2003* **2003**, *48* (4), 797−807.

https://doi.org/10.1021/acsomega.4c02439
ACS Omega 2024, 9, 24015−24024

(40) Partanen, J. I.; Juusola, P. M. Determination of Stoichiometric Dissociation Constants of Formic Acid in Aqueous Sodium or Potassium Chloride Solutions at 298.15 K. *J. Chem. Eng. Data* **2000**, *45* (1), 110−115.
(41) Fournier, P.; Oelkers, E. H.; Gout, R.; Pokrovski, G. Experimental Determination of Aqueous Sodium-Acetate Dissociation Constants at Temperatures from 20 to 240°C. *Chem. Geol.* **1998**, *151* (1), 69−84.
(42) Wypych, G.; Wypych, A. *Databook of Solvents*, 2nd ed. ChemTec Publishing, 2019.
(43) Dean, J. A.; Lange, N. A. *Lange's Handbook of Chemistry*; McGraw-Hill, 1999.
(44) Chernov, A. A. Growth Kinetics and Capture of Impurities during Gas Phase Crystallization. *J. Cryst. Growth* **1977**, *42*, 55−76.
(45) Kudryavtsev, P. G. Main Routes of the Porous Composite Materials Creation. *Nanobuild* **2020**, *12* (5), 256−269.
(46) Gilbert, D. L. Buffering of Blood Plasma. *Yale J. Biol. Med.* **1960**, *32* (5), 378−389.
(47) Ellison, G.; Straumfjord, J. V., Jr.; Hummel, J. P. Buffer Capacities of Human Blood and Plasma. *Clinical Chemistry* **1958**, *4* (6), 452−461.
(48) Bansal, V. K. Serum Inorganic Phosphorus. In *Clinical Methods: The History, Physical, and Laboratory Examinations*; Walker, H. K., Hall, W. D., Hurst, J. W., Eds.; Butterworth Publishers: Boston, 1990.

https://doi.org/10.1021/acsomega.4c02439
ACS Omega 2024, 9, 24015−24024